

# UC Berkeley

## UC Berkeley Previously Published Works

### Title

2D MOSFET operation of a fully-depleted bulk MoS<sub>2</sub> at quasi-flatband back-gate

### Permalink

<https://escholarship.org/uc/item/3wz261sg>

### Authors

Najmzadeh, M.  
Duarte, J.P.  
Khandelwal, S.  
[et al.](#)

### Publication Date

2015-06-21

Peer reviewed

## 2D MOSFET operation of a fully-depleted bulk MoS<sub>2</sub> at quasi-flatband back-gate

M. Najmzadeh, J.P. Duarte, S. Khandelwal, Y. Zeng, C. Hu

Electrical Engineering and Computer Sciences (EECS), University of California, Berkeley, 94720 CA, USA

phone: +1-510-643-1450, e-mail: [najmzadeh@berkeley.edu](mailto:najmzadeh@berkeley.edu)

In this paper, 2D MOSFET operation of a fully-depleted double-gate bulk MoS<sub>2</sub> is studied at a quasi-flatband of the back-gate for the first time. Several key device parameters such as equivalent oxide thickness (EOT), carrier concentration, flatband voltage, dielectric constant and carrier mobility were extracted from I-V and C-V characteristics and at room temperature. In a similar operation to the inversion-mode SOI MOSFETs in [1], the back-gate was used to keep a sheet of mobile charges on the flake back-side by its quasi-flatband operation at a fixed voltage (0 V). Afterward, the top-gate was used as the active gate to perform mobile charge accumulation or depletion in the channel. Fig. 1 shows the device architecture together with the high frequency R-C equivalent circuit model for this underlap gate architecture. Fig. 2 represents the top-view microscope picture of the fabricated MoS<sub>2</sub> bulk MOSFET with a flake thickness of 38 nm, measured by AFM. The fabrication steps include mechanical exfoliation of MoS<sub>2</sub> crystals on a 260 nm thick oxidized Si substrate, e-beam lithography to make S/D pads, 50 nm Ni by thermal evaporation and lift-off, gate patterning, high-k/metal-gate stack deposition (1 nm of SiO<sub>x</sub> by thermal evaporation, 11 nm of ZrO<sub>2</sub> by ALD deposition at 105 °C, 30 nm of Ni by thermal evaporation) and lift-off. The measurements were done at room temperature using an Agilent B1500A Semiconductor Parameter Analyzer. Fig. 3 shows its I<sub>d</sub>-V<sub>g</sub>, reporting a subthreshold slope of 110 mV/dec. and I<sub>on</sub>/I<sub>off</sub> of ~1×10<sup>5</sup>, both at V<sub>ds</sub>=100 mV.

**EOT, dielectric constant, flatband voltage:** Fig. 4 depicts the C<sub>g</sub>-V<sub>g</sub> measurement between the top-gate and the source-drain electrodes (V<sub>ds</sub>=0 V) at a high frequency regime (1 MHz). In strong accumulation, the EOT numeric value of the gate stack can be extracted from the maximum value of gate-channel capacitance, resulting an EOT value of 6.3 nm. In the partial depletion regime, between threshold and flatband, the gate-channel capacitance would vary by  $1/C_{gc}^2 = 1/C_{ox}^2 + 2/(q \cdot \epsilon_{ch} \cdot N_d) \cdot (V_{gs} - V_{fb})$  [2]. The flatband voltage can be extracted from the x-intercept of  $1/C_{gc}^2 - 1/C_{max}^2$ , reporting a flatband voltage of -0.45 V. The dielectric constant of the flake can be extracted from the difference in the gate-channel capacitance in strong accumulation and at the threshold voltage (-1.1 V, estimated from the linear onset of I<sub>d</sub>-V<sub>g</sub> in Fig. 3), reporting a numeric value of 7.8. This is almost in the range of the reported experimental dielectric constant numeric values in [3].

**Carrier concentration:** The carrier concentration can be extracted from the slope of  $1/C_{gc}^2 - 1/C_{max}^2$  in the linear region between threshold and flatband, reporting a value of  $2.1 \times 10^{17} \text{ cm}^{-3}$ . Note that this method can be applied to the devices with a flake thickness higher than the Debye length (~7.2 nm at this carrier concentration or doping regime).

**Series resistance:** The series resistance, similar to an inversion-mode MOSFET in [4], can be extracted from the y-intercept of R<sub>tot</sub>=V<sub>ds</sub>/I<sub>d</sub> vs. 1/(V<sub>gs</sub>-V<sub>fb</sub>) in linear accumulation regime (V<sub>ds</sub><V<sub>gs</sub>-V<sub>fb</sub>), see Fig. 4, assuming accumulation as the dominant conduction mechanism in comparison to bulk conduction. This assumption is justified considering the channel accumulation conductance ( $\mu \cdot C_{ox} \cdot W/L \cdot (V_{gs} - V_{fb})$ ) of three times higher than the bulk conductance at flatband ( $q \cdot \mu \cdot N_d \cdot t \cdot W/L$ ). An almost similar mobility assumption for bulk and accumulation conduction results a bias range of V<sub>gs</sub>-V<sub>fb</sub>>0.60 V. A series resistance of 434 kΩ is extracted in Fig. 4, while this fairly high value is due to the used underlap gate design to minimize the parasitic gate-source and drain capacitances. Note that Benzyl Viologen (BV) [5] or SiN<sub>x</sub> [6] doping can be performed in the S/D extensions to suppress such resistances as well as minimize their gate-bias-dependencies especially above flatband and for shorter lengths [7].

**Carrier mobility:** The effective carrier mobility can be extracted using the split C-V method, similar to a junctionless/accumulation-mode device in [8]-[9], covering a wide gate voltage range from threshold to strong accumulation ( $\mu_{eff} = I_d \cdot L / (W \cdot Q_n \cdot V_{ds})$ ;  $Q_n = \int_{off}^{V_g} C_{gc} \cdot dV_g$ ). Q<sub>n</sub> is the normalized mobile negative charges in the channel per unit area. Fig. 5 shows the numeric effective mobility values after the series resistance correction, reporting a maximum effective electron mobility value of 48 cm<sup>2</sup>/V.s. For comparison, the effective mobility is also extracted from I-V characteristics, after a series resistance correction and from the g<sub>m</sub> values in linear accumulation regime,  $\mu_{eff} = g_m / (C_{ox} \cdot W/L \cdot V_{ds})$ , reporting a maximum numeric value of 26 cm<sup>2</sup>/V.s. The slight effective mobility underestimation using only I-V characteristics can be due to neglecting the bias-dependency of the gate-channel capacitance in strong accumulation regime.

**Conclusion and further works:** In this work, we extracted several device parameters in a double-gate bulk MoS<sub>2</sub> MOSFET using C-V and I-V characteristics. Such device extraction methodologies were done assuming a typical linear operation of an accumulation-mode MOSFET from depletion to accumulation. This parameter extraction platform can be used to investigate the possible bias-dependency of key material parameters e.g. dielectric constant and bandgap [10], in a high normal electric field considering a back-gate operation. This includes incorporation of photoluminescence measurement on direct bandgap 2D devices, monolayer e.g. MoS<sub>2</sub> and bulk e.g. ReS<sub>2</sub> [11] as well

as additional measurement methods e.g. Hall for comparison of e.g. mobility and carrier concentration values.  
 This work was supported by ATMI Inc. within the i-Rice program.

[1] J. Chen et al., IEEE EDL 1991.  
 [2] Y. Taur et al., Fundamentals of modern VLSI devices, Cambridge University Press, 2009.  
 [3] X. Chen et al., Nature Communications 2015.  
 [4] M. Najmzadeh et al., IEEE TNANO 2012.  
 [5] D. Kiriya et al., J. Am. Chem. Soc. 2014.

[6] K. Chen et al., APL Mat. 2014.  
 [7] M. Najmzadeh et al., SSE 2014.  
 [8] C.G. Sodini et al., SSE 1982.  
 [9] T. Rudenko et al., APL 2012.  
 [10] E.J.G. Santos et al., ACS Nano 2013.  
 [11] S. Tongay et al., Nature Communications 2014.

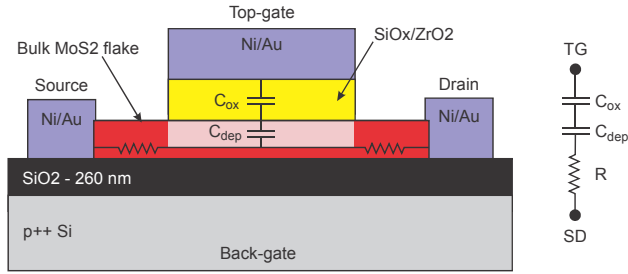


Fig. 1: The device architecture, showing a top-gate operation between threshold and flatband voltage (left) and a high frequency model of the device (right).

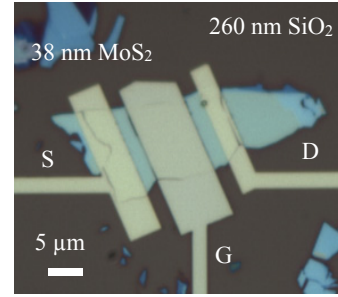


Fig. 2: The top-view microscope picture of the measured underlap top-gate MoS<sub>2</sub> MOSFET.

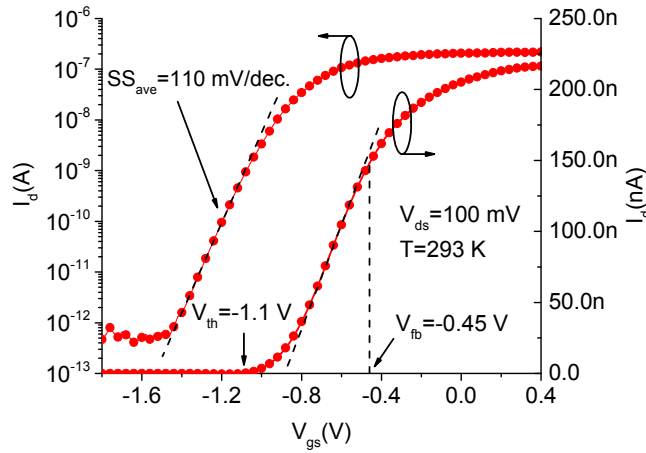


Fig. 3:  $I_d$ - $V_g$  characteristics at  $V_{ds}=100$  mV and  $V_{bg}=0$  V.

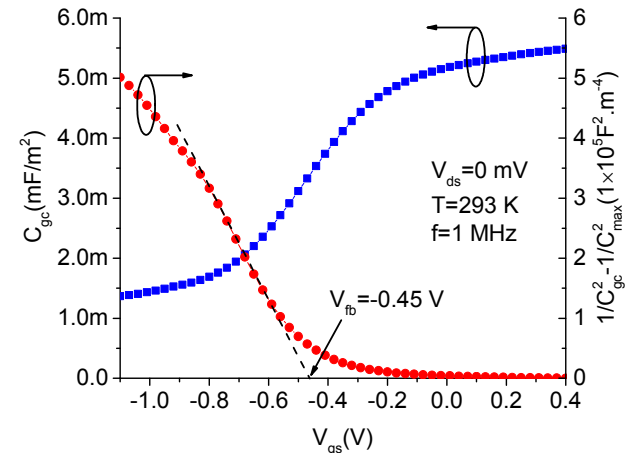


Fig. 4:  $C_{gc}$ - $V_g$  characteristics at 1 MHz and  $V_{ds}=0$  V.

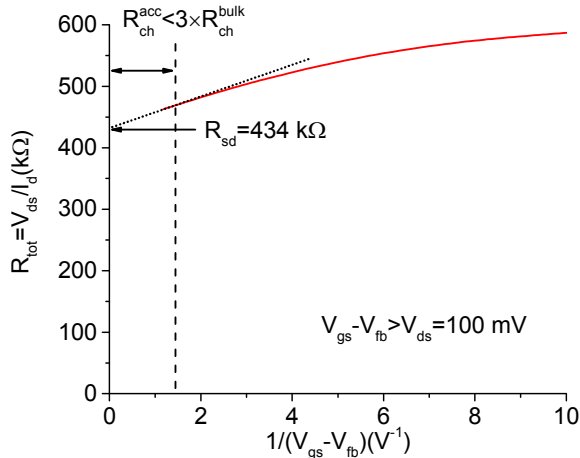


Fig. 5: Extraction of series resistance in linear accumulation regime from the total source-drain resistance vs.  $1/(V_{gs}-V_{fb})$ .

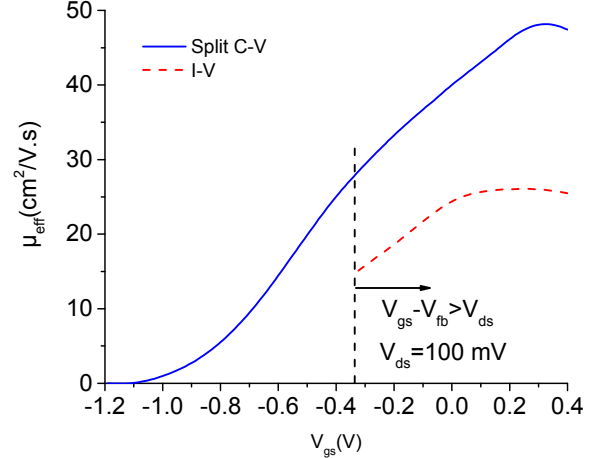


Fig. 6: Effective mobility extraction using split-CV and I-V, after series resistance correction.